

# Evaluation of Stochastic Gradient Descent Optimizer on U-Net Architecture for Brain Tumor Segmentation

Purwono <sup>a,1,\*</sup>, Iis Setiawan Mangkunegara <sup>b,2</sup>

<sup>a</sup> Department of Informatics, Universitas Harapan Bangsa, Purwokerto 53182, Indonesia

<sup>b</sup> Department of Information Technology, Universitas Harapan Bangsa, Purwokerto 53182, Indonesia

<sup>1</sup> [purwono@uhb.ac.id](mailto:purwono@uhb.ac.id); <sup>2</sup> [iissmn@uhb.ac.id](mailto:iissmn@uhb.ac.id)

\* Corresponding Author

## ARTICLE INFO

### Article history

Received July 21, 2023

Revised August 05, 2023

Accepted August 18, 2023

### Keywords

SGD;

U-Net;

Segmentation;

Brain Tumor;

Optimization

## ABSTRACT

A brain tumor is a type of disease that is quite dangerous in the world. This disease is one of the main causes of human death and has a high risk of recurrence. There are several types of brain tumor locations such as edema, necrosis to elevation. Segmenting the location of this disease is important to do to support faster recovery efforts. The Convolutional Neural Network (CNN) algorithm, which is part of the deep learning method, can be an alternative to this segmentation effort. The U-Net architecture is part of the CNN algorithm which specifically works on medical image segmentation. This study experimented to build a special U-Net architecture for medical image segmentation that had been optimized with SGD. The data used is BraTS20200 which contains a collection of MRI data. This optimization aims to improve the performance of the U-net architecture for segmenting brain tumor images. The results of the study show that the SGD optimization carried out has succeeded in providing better performance than previous studies. This can be seen from the performance value obtained at 0.9879. This accuracy value indicates an increase in accuracy from previous studies. High accuracy indicates that the SGD-optimized model has good segmentation prediction performance.

This is an open-access article under the [CC-BY-SA](https://creativecommons.org/licenses/by-sa/4.0/) license.



## 1. Introduction

A brain tumor is a type of disease with an estimated 29.9 million adult sufferers per year [1]. This disease is one of the leading causes of death in the world and has a higher risk of recurrence even though standard treatment has been used [2]. Abnormal tissue growth resulting from uncontrolled cell multiplication leads to the development of brain tumors [3].

Glioma is the most common brain tumor and originates from the glial. Based on WHO data, there are several classifications of this disease from grade I to grade IV [4]. Grades I and II are considered low-grade gliomas (LGG) which are less aggressive and have a longer life expectancy of several years. [4]. Grades III and IV are considered high-grade glioma (HGG) with a higher degree of aggressiveness and their patients have an average life expectancy of less than 2 years [5]. To prevent deteriorating health, a person's quality of life must be maintained to maintain a better life [6].

Brain tumor segmentation is a challenging and very important task in the medical field [7]. Accurate and automatic segmentation of brain tumors is very important as a clinical diagnosis [8].

The segmentation process is considered a challenging task because the shape, size, and location of brain tumors vary among different types of patients [9]. Segmentation techniques can be carried out by utilizing a medical image approach with artificial intelligence technology, namely deep learning.

Within the medical field, deep learning has made significant and rapid advancements in processing and analyzing image data [10]. Deep learning has shown quite rapid progress and shows better performance improvements in various computer vision problems [11]. Deep learning has been widely used in the task of segmenting brain tumor images from MRI (Magnetic Resonance Imaging) data and shows excellent performance in segmenting all tumor tissue [12]. Segmenting the location of a disease is important to support faster recovery efforts. The Convolutional Neural Network (CNN) algorithm, which is part of the deep learning method, can be an alternative to this segmentation effort [13]. The U-Net architecture is part of the CNN algorithm which specifically works on medical image segmentation.

One of the deep learning algorithms that can be used in medical image segmentation is U-net. The U-net model has shown much greater potential for the medical image segmentation task [14]. U-net is the first architecture used for 2D image segmentation [15]. Until now, U-net has also been developed in 3D imagery [16]. The U-net consists of two lines, namely the encoder line and the decoder line. The encoder path is used as a tool to capture the context of the image while the decoder path is used to expand to the size of the original image. In the medical field, U-Net is often used for medical image segmentation [17].

Numerous prior researchers have carried out similar studies, utilizing U-Net as a method for segmenting brain tumors. Research conducted by Walsh [18] namely proposing a lightweight U-Net model that can segment MRI scans in real-time and does not require additional data augmentation. The results of this study achieve an intersection-over-union (IoU) average of 89% which outperforms the standard benchmark algorithm. Li [19] has also conducted related research in the same area namely segmenting brain tumors from MRI data with U-Net. The results of this study are to obtain DSC metric values of 0.890, 0.842, and 0.835 for all segmentation areas, respectively. Doctors have also endorsed the performance of this research.

The deep learning framework that is very popular in use is *Keras*. This framework has several optimizers that can be used to update network weights based on the loss function [20]. The optimizer is in charge of minimizing errors or differences between predictions and targets [21]. Based on several previous studies, there has been no attempt by researchers to implement the U-Net architecture SGD optimizer for brain tumor image segmentation. This research generally contributes to the evaluation efforts of the SGD optimizer from the training process to testing. SGD optimization has the advantage of being a simple technique but able to shorten update time when handling many samples and can eliminate computational duplication. This makes SGD optimization able to accelerate computation in deep learning [22]. The results of this performance can be used as a reference in choosing the right optimizer when segmenting medical images. This can support in adding insight into knowledge of health information [23].

## 2. Method

### 2.1. Dataset

The dataset used is sourced from secondary data, namely the BraTS2020 Dataset (Training + Validation) which can be downloaded freely on the Kaggle site in the "nii" format [24]. The dataset is in the form of a collection of brain tumor images from MRI data. The data comes from a radiological scanning technique that uses magnets, radio waves, and a computer to produce images of body structures [25]. There are several different settings for this MRI data, namely T1: T1-weighted 2D acquisition, original image, sagittal or axial, with a slice thickness of 1–6 mm. T1c refers to a contrast-enhanced (Gadolinium) image using a 3D acquisition and 1 mm isotropic voxel size for the majority of patients in T1-weighted imaging. T2: Axial 2D acquisition of T2-weighted images with a slice thickness ranging from 2 to 6 mm. FLAIR: Axial, coronal, or sagittal 2D acquisition of T2-weighted

FLAIR images with a slice thickness of 2 to 6 mm. The data presented in Fig. 1 has been validated. All imaging data sets were manually segmented by one to four assessors, following a consistent annotation protocol, and these annotations were approved by experienced neuroradiologists. Annotations consist of GD enhancing tumor (ET — label 4), peritumoral edema (ED — label 2), and necrotic tumor core (NCR/NET — label 1). Edema indicates a collection of fluid above the water. Necrosis indicates the accumulation of dead cells and is best seen on the T1 post-contrast sequence. Enhancing shows blood brain barrier damage and is seen on T1c post-contrast sequencing. Non-enhancing is an area that is not in the area of edema, necrotic, or enhancing tumor. The dataset used is a public dataset with a license CC0: Public Domain. This data certainly will not violate research ethics.

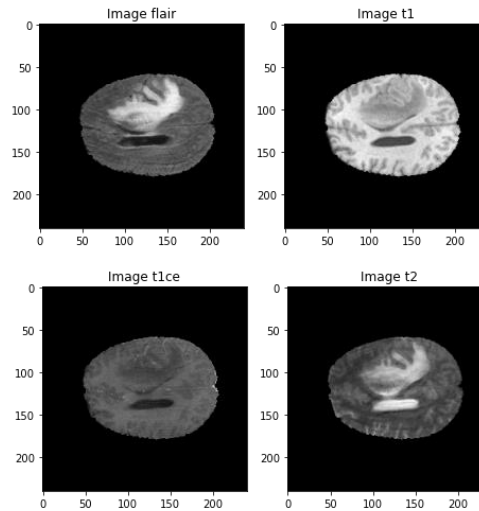


Fig. 1. Brain Tumor Dataset

## 2.2. Image Preprocessing

Data processing is an important step before data can be applied to machine learning [26]. This step is used to ensure that the data is of good quality when used to train the model [27]. Preprocessing involves cleansing raw data and getting it ready for input into an algorithm [28]. The image data generator is used in processing the brain tumor MRI dataset. This technique can cope with small dataset sizes and generate additional tens of thousands of images [29]. In the image data generator, we use the image augmentation technique which is a technique of applying different transformations to the original image resulting in multiple transform copies of the same image [30][31]. However, each copy differs from the other in certain aspects depending on the augmentation techniques applied such as panning, rotating, flipping, and so on [32]. Input images are processed by converting them into floating-point tensors into deep learning models. The stages used in this processing are (1) reading image files stored in folders, (2) decoding JPEG content into an RGB pixel grid with channels, (3) converting it into a floating-point tensor as input data to the model, (4) scales pixel values (between 0 and 255) to [0,1] intervals. The flow of image processing can be seen in Fig. 2.

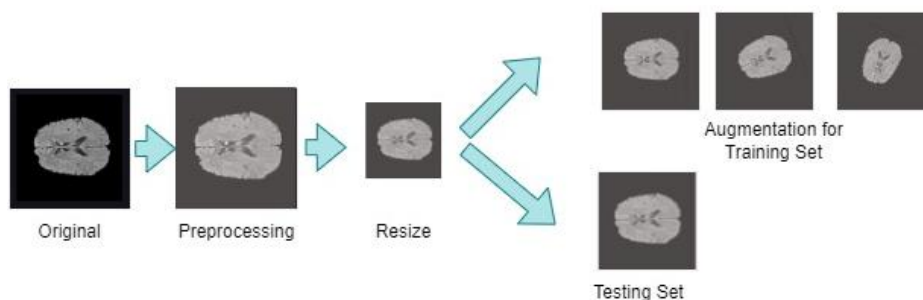


Fig. 2. Image Processing

### 2.3. U-Net Model

U-Net is a popular convolutional network-based semantic segmentation model extensively utilized in the medical domain. U-Net can produce good predictions even with little training data [29]. The U-Net segmentation model is a classic encoder-decoder structure which can be seen in Fig. 3.

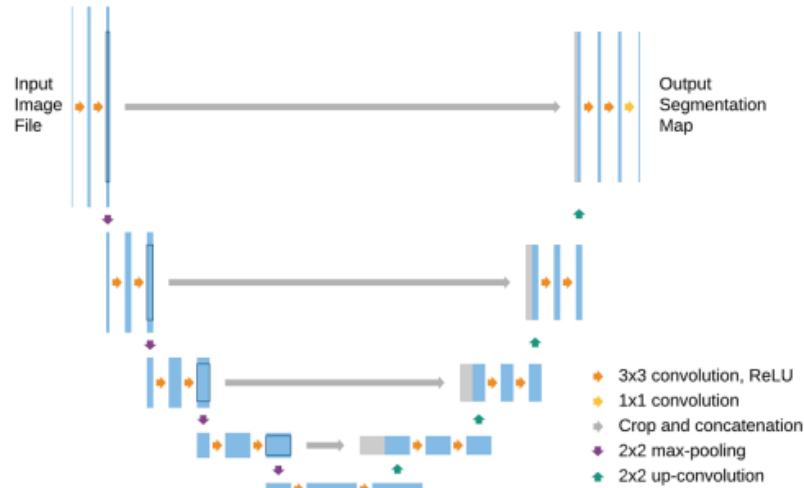


Fig. 3. U-Net Architecture

Each block in the U-Net is on a contract path consisting of two consecutive  $3 \times 3$  convolutions followed by the ReLU activation unit and the max-pooling layer [33]. This configuration is iterated multiple times. It involves an expansive path that enlarges the sample feature map using  $2 \times 2$  up-convolution. Then, the feature map from the corresponding layer in the contracting path is cropped and combined with the feature map. Afterward, two consecutive  $3 \times 3$  convolutions with ReLU activation are applied. The final stage in U-Net includes a  $1 \times 1$  convolution, which reduces the feature map to the desired number of channels, resulting in segmented images. Pruning at the edge of the feature map is necessary because the amount of contextual information is the least, so it needs to be removed. This process creates a U-shaped grid, allowing objects to be grouped within an area by utilizing the context of the larger overlapping region. The corresponding equation is presented in Equation (1).

$$E = \sum w(x) \log(p_{k(x)}(x)) \quad (1)$$

Where  $p_k$  is the pixel-based softmax function that is applied to the final feature map defined in Equation (2).

$$p_k = \exp(a_k(x)) / \sum_{k'=1}^k \exp(a_{k'}(x)) \quad (2)$$

Where  $a_k$  indicates activation on the  $k$  channel.

U-Net is the most typical type of deep learning used in medical image segmentation [34]. U-Net is an architecture that is mathematically simple and easy to implement. Due to its simplicity and versatility, this approach becomes highly appealing for implementation across diverse medical imaging domains, including ultrasound, X-ray, nuclear magnetic resonance, and nuclear medical imaging [35].

### 2.4. Loss Function

Loss functions are generally used to optimize a deep learning model [36]. Loss means prediction errors by the algorithm while the way to calculate the loss is a function. The loss function method used

in this study is the dice coefficient. This method can be used to calculate sample similarity [37]. The formula used can be seen in the Equation (3).

$$Dice(D, Q) = \frac{2|D \cap Q|}{|D| + |Q|} \quad (3)$$

Where  $D$  ( $D, Q$ ) is similarity value between sets  $D$  and sets  $Q$ ,  $|D \cap Q|$  is the number of elements that are the same between set  $D$  and set  $Q$ ,  $|D|$  is how many elements are in set  $D$ , and  $|Q|$  is how many elements are in set  $Q$ .

The dice coefficient has found extensive application in MRI image segmentation [38]. This technique can be employed to assess the pixel match between the predicted segmentation and the corresponding ground truth [39]. In image segmentation, the dice coefficient is 2 times the overlap area divided by the total number of pixels in both images. This dice coefficient is applied to several types of annotations which will produce dice coefficient enhancing, edema, and necrotic.

In this research, we also created a function to calculate precision, sensitivity, and specificity values. Precision is the proportion of accurately predicted positive outcomes relative to the total positive predictions made [40][41]. Sensitivity is the fraction of accurately predicted positive outcomes concerning the entirety of correctly positive data [42][43]. Specificity refers to the accuracy of predicting a negative outcome in comparison to the total negative data [44].

## 2.5. SGD Optimizer

The optimizer acts as an optimizer by updating the weight parameters and then minimizing the loss function [45]. Before training the model, the optimizer must be selected along with its hyperparameters. Several types of optimizers can be used, namely Adam, SGD, Adadelata, Nadam, and Adamax. Adam is an algorithm derived from the classic SGD algorithm, featuring updated network weights [20]. Adadelata, known as an adaptive learning rate algorithm, automatically adjusts the learning rate to optimize the stochastic gradient descent algorithm, resulting in improved prediction accuracy [46]. Nadam has been applied as an optimizer for the stochastic gradient descent method. Moreover, during training, validation data arguments in the model have been utilized to maintain training and test loss traces. Nadam's functionality is a step ahead of Adam's and has successfully reduced RMSE errors [47]. The AdaMax method uses the maximum value of the second part momentum calculation method on ADAM. This provides a more stable method [48].

SGD is a basic algorithm and is widely used in machine learning algorithms. Instead of calculating gradients on all training examples and updating the weights, SGD updates the weights for each training [49]. Gradient Descent is one of the iterative optimization algorithms to find the point that minimizes a function that can be derived [50]. This method works by starting from an initial guess and iteratively this guess can be corrected based on a rule involving the gradient/first derivative of the function you want to minimize. Equation (4) is used in cases that specifically regulate the steps taken to derive the function to be minimized.

$$\omega_i + 1 = \omega_i - \eta_{\omega_i} L(\omega_i) \quad (4)$$

Where  $\omega_i + 1$  are model parameters for prediction,  $\omega_i$  is the model parameter from the preceding iteration,  $\eta$  Is the learning rate, and  $L$  represents the loss cost function. In the standard Gradient Descent learning phase, calculating derivatives for all samples in the training dataset at each iteration is necessary. However, this can lead to computational intensity when dealing with large training data. SGD, a variant of Gradient Descent, randomly selects a single training sample at a time for training. This approach is more scalable and faster to train, with no time constraints on execution regardless of the training dataset's size.

## 2.6. Model Training

The training process for medical image segmentation uses a model built using the U-Net architecture. In this study, there are three parameters used in making the U-net model, namely input,

kernel\_initializer, and dropout. The input data is the medical image which will be segmented and positioned on the input layer. The kernel initializer is the distribution used to initialize the W weights for each input. Dropout is a neural network regularization method in which certain neurons are randomly chosen and excluded from training [44]. In this study, the input is a shape tensor filled with the parameters image\_height, image\_width, and color\_channels. The activation function used is Relu. The kernel used is he\_normal and has a dropout of 0.5.

Models built with the U-Net architecture have encoders and decoders. The encoder section applies a convolution block followed by maxpool downsampling which is in charge of encoding the medical image input in feature representation at various levels. The decoder section is in charge of projecting features at a semantically lower resolution. This part consists of upsampling and concatenation followed by regular convolution operations.

The training process for this model is applied to the previously created loss function to produce several evaluation results such as dice coefficient, necrotic dice coefficient, dice coefficient edema, dice coefficient enhancing, precision, sensitivity, specificity, and accuracy. The accuracy measurement used in this training model utilizes the intersection over union (IoU) method as a step to detect an object. Intersection over Union (IoU) is utilized to assess the performance of object detection by comparing the bounding box from the ground truth with the predicted bounding box [51]. The U-Net model created for this research will subsequently employ the outcomes of the implemented SGD optimizer.

## 2.7. Model Testing

The training stage plays an active role so that the model can predict brain tumor segmentation well from the image data set that has been previously trained. To find out how well it performs this segmentation, the testing process must be carried out. This test will also produce an evaluation value from the experimental use of the model on the test data. The prediction process in this test will show the stages of image segmentation from original image flair, ground truth, all classes, necrotic, edema, and enhancing. Evaluation of the model will also produce values for accuracy, dice coefficient, sensitivity, specificity, and precision. U-net relies on large amounts of data to prevent overfitting [52]. This event refers to the accuracy of the training model as if it produces a perfect score. This study utilizes augmentation techniques in data preprocessing to overcome the problem of limited datasets with small numbers.

## 3. Experimental Results

### 3.1. Data Preprocessing

Preprocessing is a process that is carried out before entering the training model stage. In this process, digital images are processed to obtain better image quality and optimal results when the data is processed during the training model [31]. Based on the data that has been processed using a data generator, namely image augmentation, we have succeeded in making data that is feasible to be input data for the U-Net architecture.

### 3.2. Model Training

The U-net model built in this study was optimized with SGD. A total of 35 epochs have been used as iterations in this training process. The visualization of the training process that has been carried out can be seen in Fig. 4. Based on Fig. 4, the training process that is run produces several values such as accuracy, loss, dice coefficient, and mean IoU. The accuracy generated in this training process is considered quite good because it gets an average IoU accuracy validation value above 99%, and the loss value continues to decrease. Loss function values that continue to decrease indicate that the model has worked quite well. The dice coefficient value generated during training is 0.645983. The similarity value is good enough but still needs to be improved again to get maximum test results. The model is then saved to perform medical image segmentation prediction work from the prepared test dataset.

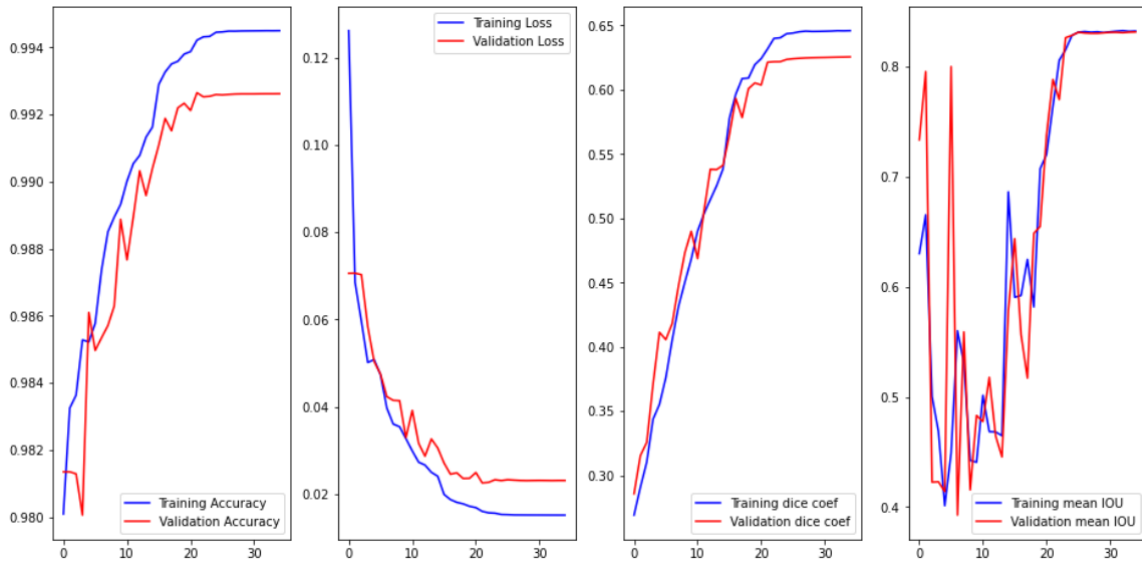


Fig. 4. Model Training

### 3.3. Model Prediction

The U-Net mode which has been optimized with SGD is then assigned to detect brain tumor image segmentation from testing data based on predetermined dataset locations. This prediction process is carried out to find out how well the model is in testing segmentation. Several brain tumor images will be tested in this segmentation. Testing this prediction will see several annotations on part of the image such as necrotic, edema, and enhancement from the original image. Fig. 5 is an example of the prediction results of annotation segmentation with a model that has been previously trained.

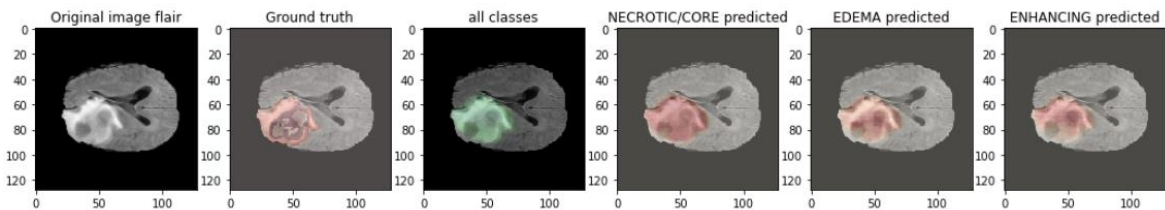


Fig. 5. Model Prediction

The results of the annotation segmentation that has been successfully carried out, then predict the class of brain tumor segmentation. We have used 4 classes in this segmentation namely not tumor, necrotic, edema, and enhancing. The further annotation process produces a segmentation image from the semantic techniques commonly produced by the U-Net model. Fig. 6 is an example of the class prediction process from image segmentation that has been done.

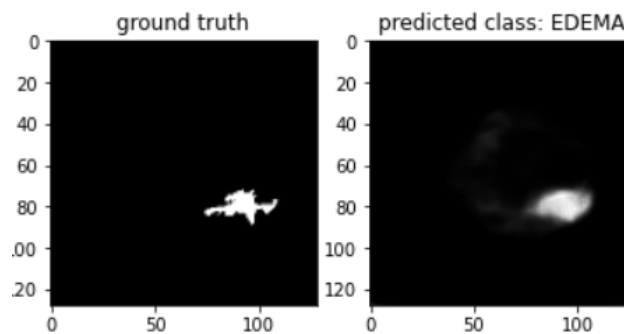


Fig. 6. Brain Tumor Class Segmentation

Based on Fig. 6, it can be seen that the model that has been built is successful in segmenting brain tumor images based on their class. Evaluation of the testing model is carried out to obtain the value of the accuracy of the test, the dice coefficient of each class, precision, sensitivity, and specificity. This evaluation uses loss in the form of categorical entropy because we use multi classes. Table 1 is the result of an evaluation of the model that has been made on the test data.

**Table 1.** Model Evaluation Result

Metric	Value
Accuracy	0.9879
Dice Coefficient	0.3638
Dice Coefficient Necrotic	0.2236
Dice Coefficient Edema	0.4044
Dice Coefficient Enhancing	0.2921
Precision	0.9937
Specificity	0.9977
Sensitivity	0.9829

Based on Table 1, the accuracy value generated at this test stage has a value of 0.9879. The results of this study have a higher accuracy value than Walsh and Li's research which has an accuracy of 0.89. However, when compared to the Sangui study with an accuracy value of 0.994, the accuracy value produced in this study tends to be lower. In this study, we found the results that there is a dice coefficient value that can be said to have a similarity value that is not maximized where it has not reached a value above 0.5. This is of course a decrease in performance in detecting similarity compared to the training model that has been made. In contrast to Yaqub's research [53] which used the Adam optimizer with an accuracy value of 0.992, this study still has superior accuracy.

#### 4. Conclusion

The U-Net architecture, which is commonly applied in medical image segmentation, usually shows commendable accuracy performance. Optimization carried out with stochastic gradient descent gives a higher accuracy value than previous studies. This study has an accuracy of 0.9878 which indicates that the model has worked well in segmenting brain tumor images. The test results of this model have succeeded in predicting the specified segmentation class. In the future, it is necessary to conduct experiments on different medical image datasets to find out the performance of this model. Further research also needs to be done by comparing the performance of several other optimizers or a combination of several optimizers in deep learning. A comparison of the performance of other optimizers needs to be done so that the training model created produces a more effective and efficient model. The results of quite good accuracy from SGD optimization can certainly be the basis for decisions by medical personnel in making intelligent systems in the field of medical image segmentation. Apart from the advantages of optimizing the SGD that has been implemented, of course, some limitations certainly need to be reviewed so that it deserves to be called a deep learning model that can be used in health technology.

**Author Contribution:** All authors contributed equally to the main contributor to this paper. All authors read and approved the final paper.

**Funding:** This research received no external funding.

**Conflicts of Interest:** The authors declare no conflict of interest.

#### References

- [1] J. Wu *et al.*, "TISS-net: Brain tumor image synthesis and segmentation using cascaded dual-task networks and error-prediction consistency," *Neurocomputing*, vol. 544, p. 126295, 2023,

- <https://doi.org/10.1016/j.neucom.2023.126295>.
- [2] T. Zhou *et al.*, "Prediction of brain tumor recurrence location based on multi-modal fusion and nonlinear correlation learning," *Comput. Med. Imaging Graph.*, vol. 106, p. 102218, 2023, <https://doi.org/10.1016/j.compmedimag.2023.102218>.
- [3] M. Nazir, S. Shakil, and K. Khurshid, "Role of deep learning in brain tumor detection and classification (2015 to 2020): A review," *Comput. Med. Imaging Graph.*, vol. 91, p. 101940, 2021, <https://doi.org/10.1016/j.compmedimag.2021.101940>.
- [4] D. N. Louis *et al.*, "The 2021 WHO Classification of Tumors of the Central Nervous System: a summary.," *Neuro. Oncol.*, vol. 23, no. 8, pp. 1231–1251, Aug. 2021, <https://doi.org/10.1093/neuonc/noab106>.
- [5] S. Lefkovits and L. Lefkovits, "U-Net architecture variants for brain tumor segmentation of histogram corrected images," *Acta Univ. Sapientiae, Inform.*, vol. 14, no. 1, pp. 49–74, 2022, <https://doi.org/10.2478/ausi-2022-0004>.
- [6] M. Elizabeth and C. Baua, "Quality of Life, Social Support, and Physical Activity of Overweight Adolescents," *J. Adv. Heal. Informatics Res.*, vol. 1, no. 2, pp. 58–64, 2023, <https://doi.org/10.59247/jahir.v1i2.32>.
- [7] T. Ruba, R. Tamilselvi, and M. Parisa Beham, "Brain tumor segmentation using JGate-AttResUNet – A novel deep learning approach," *Biomed. Signal Process. Control*, vol. 84, p. 104926, 2023, <https://doi.org/10.1016/j.bspc.2023.104926>.
- [8] Z. Ullah, M. Usman, M. Jeon, and J. Gwak, "Cascade multiscale residual attention CNNs with adaptive ROI for automatic brain tumor segmentation," *Inf. Sci. (Ny)*, vol. 608, pp. 1541–1556, 2022, <https://doi.org/10.1016/j.ins.2022.07.044>.
- [9] Y. Li, Z. Yuan, J. Wang, and Q. Xu, "Laser-induced damage characteristics in fused silica surface due to mechanical and chemical defects during manufacturing processes," *Opt. Laser Technol.*, vol. 91, pp. 149–158, 2017, <https://doi.org/10.1016/j.optlastec.2016.12.022>.
- [10] T. Zhou, Q. Cheng, H. Lu, Q. Li, X. Zhang, and S. Qiu, "Deep learning methods for medical image fusion: A review," *Comput. Biol. Med.*, vol. 160, p. 106959, 2023, <https://doi.org/10.1016/j.compbiomed.2023.106959>.
- [11] M. Havaei *et al.*, "Brain tumor segmentation with Deep Neural Networks," *Med. Image Anal.*, vol. 35, pp. 18–31, 2017, <https://doi.org/10.1016/j.media.2016.05.004>.
- [12] X. Li, G. Luo, and K. Wang, "Multi-step Cascaded Networks for Brain Tumor Segmentation," in *Brainlesion: Glioma, Multiple Sclerosis, Stroke and Traumatic Brain Injuries*, 2020, pp. 163–173, [https://doi.org/10.1007/978-3-030-46640-4\\_16](https://doi.org/10.1007/978-3-030-46640-4_16).
- [13] K. U. Wijaya and E. B. Setiawan, "Hate Speech Detection Using Convolutional Neural Network and Gated Recurrent Unit with FastText Feature Expansion on Twitter," *J. Ilm. Tek. Elektro Komput. dan Inform.*, vol. 9, no. 3, pp. 619–631, 2023, <http://dx.doi.org/10.26555/jiteki.v9i3.26532>.
- [14] H. Zhang *et al.*, "BCU-Net: Bridging ConvNeXt and U-Net for medical image segmentation," *Comput. Biol. Med.*, vol. 159, p. 106960, 2023, <https://doi.org/10.1016/j.compbiomed.2023.106960>.
- [15] R. Gamal, H. Barka, and M. Hadhoud, "GAU U-Net for multiple sclerosis segmentation," *Alexandria Eng. J.*, vol. 73, pp. 625–634, 2023, <https://doi.org/10.1016/j.aej.2023.04.069>.
- [16] J. C. González Sánchez, M. Magnusson, M. Sandborg, Å. Carlsson Tedgren, and A. Malusek, "Segmentation of bones in medical dual-energy computed tomography volumes using the 3D U-Net," *Phys. Medica*, vol. 69, pp. 241–247, 2020, <https://doi.org/10.1016/j.ejmp.2019.12.014>.
- [17] Z. Wang, Y. Zou, and P. X. Liu, "Hybrid dilation and attention residual U-Net for medical image segmentation," *Comput. Biol. Med.*, vol. 134, p. 104449, 2021, <https://doi.org/10.1016/j.compbiomed.2021.104449>.
- [18] J. Walsh, A. Othmani, M. Jain, and S. Dev, "Using U-Net network for efficient brain tumor segmentation in MRI images," *Healthc. Anal.*, vol. 2, p. 100098, 2022, <https://doi.org/10.1016/j.health.2022.100098>.
- [19] P. Li, W. Wu, L. Liu, F. Michael Serry, J. Wang, and H. Han, "Automatic brain tumor segmentation from Multiparametric MRI based on cascaded 3D U-Net and 3D U-Net++," *Biomed. Signal Process. Control*, vol. 78, p. 103979, 2022, <https://doi.org/10.1016/j.bspc.2022.103979>.
- [20] J. Ott, M. Pritchard, N. Best, E. Linstead, M. Curcic, and P. Baldi, "A Fortran-Keras deep learning bridge for scientific computing," *Scientific Programming*, vol. 2020, pp. 1-13, 2020, <https://doi.org/10.1155/2020/8888811>.
- [21] E. Haghghat and R. Juanes, "SciANN: A Keras/TensorFlow wrapper for scientific computations and physics-informed deep learning using artificial neural networks," *Computer Methods in Applied Mechanics and Engineering*, vol. 373, p. 113552, <https://doi.org/10.1016/j.cma.2020.113552>.
- [22] Y. Tian, Y. Zhang, and H. Zhang, "Recent Advances in Stochastic Gradient Descent in Deep Learning,"

- Mathematics*, vol. 11, p. 682, 2023, <https://doi.org/10.3390/math11030682>.
- [23] M. Muflih, R. Widaryanti, F. L. Indrawati, and N. G. Trisagita, "Correlation Between Knowledge of Health Information About Picky Eating, Supplementary Feeding, Management Ability of Appetite Herbs," *J. Adv. Heal. Informatics Res.*, vol. 1, no. 2, pp. 65–74, 2023, <https://doi.org/10.59247/jahir.v1i2.34>.
- [24] S. Sangui, T. Iqbal, P. C. Chandra, S. K. Ghosh, and A. Ghosh, "3D MRI Segmentation using U-Net Architecture for the detection of Brain Tumor," *Procedia Comput. Sci.*, vol. 218, pp. 542–553, 2023, <https://doi.org/10.1016/j.procs.2023.01.036>.
- [25] D. C. E. Saputra, Y. Maulana, T. A. Win, R. Phann, and W. Caesarendra, "Implementation of Machine Learning and Deep Learning Models Based on Structural MRI for Identification Autism Spectrum Disorder," *J. Ilm. Tek. Elektro Komput. dan Inform.*, vol. 9, no. 2, pp. 307–318, 2023, <http://dx.doi.org/10.26555/jiteki.v9i2.26094>.
- [26] I. S. Mangkunegara and P. Purwono, "Analysis of DNA Sequence Classification Using SVM Model with Hyperparameter Tuning Grid Search CV," in *2022 IEEE International Conference on Cybernetics and Computational Intelligence (CyberneticsCom)*, 2022, pp. 427–432, <https://doi.org/10.1109/CyberneticsCom55287.2022.9865624>.
- [27] R. Nyirandayisabye, H. Li, Q. Dong, T. Hakuzweyezu, and F. Nkinahamira, "Automatic pavement damage predictions using various machine learning algorithms: Evaluation and comparison," *Results Eng.*, vol. 16, p. 100657, 2022, <https://doi.org/10.1016/j.rineng.2022.100657>.
- [28] D. Arifah, T. H. Saragih, D. Kartini, and M. I. Mazdadi, "Application of SMOTE to Handle Imbalance Class in Deposit Classification Using the Extreme Gradient Boosting Algorithm," *J. Ilm. Tek. Elektro Komput. dan Inform.*, vol. 9, no. 2, pp. 396–410, 2023, <http://dx.doi.org/10.26555/jiteki.v9i2.26155>.
- [29] M. Ahmad *et al.*, "Industry 4.0 technologies and their applications in fighting COVID-19 pandemic using deep learning techniques," *Comput. Biol. Med.*, vol. 145, p. 105418, 2022, <https://doi.org/10.1016/j.compbiomed.2022.105418>.
- [30] N. N., "Early identification of Alzheimer's Disease using medical imaging: A review from a machine learning approach perspective," *J. Ilm. Tek. Elektro Komput. dan Inform.*, vol. 9, no. 3, 2023, <http://dx.doi.org/10.26555/jiteki.v9i3.25148>.
- [31] D. A. Pramudhita, F. Azzahra, I. K. Arfat, R. Magdalena, and S. Saidah, "Strawberry Plant Diseases Classification Using CNN Based on MobileNetV3-Large and EfficientNet-B0 Architecture," *J. Ilm. Tek. Elektro Komput. dan Inform.*, vol. 9, no. 3, pp. 522–534, 2023, <http://dx.doi.org/10.26555/jiteki.v9i3.26341>.
- [32] B. D. Satoto, R. T. Wahyuningrum, and B. K. Khotimah, "Classification of Corn Seed Quality Using Convolutional Neural Network with Region Proposal and Data Augmentation," *J. Ilm. Tek. Elektro Komput. dan Inform.*, vol. 9, no. 2, pp. 348–362, 2023, <http://dx.doi.org/10.26555/jiteki.v9i2.26222>.
- [33] N. Siddique, S. Paheding, C. P. Elkin, and V. Devabhaktuni, "U-net and its variants for medical image segmentation: A review of theory and applications," *IEEE Access*, pp. 82031–82057, 2021, <https://doi.org/10.1109/ACCESS.2021.3086020>.
- [34] C. Li, X. Li, and R. Zhou, "Cochlear CT image segmentation based on u-net neural network," *J. Radiat. Res. Appl. Sci.*, vol. 16, no. 2, p. 100560, 2023, <https://doi.org/10.1016/j.jrras.2023.100560>.
- [35] R. Li *et al.*, "A novel U-Net based data-driven vanadium redox flow battery modelling approach," *Electrochim. Acta*, vol. 444, p. 141998, 2023, <https://doi.org/10.1016/j.electacta.2023.141998>.
- [36] H. Bai, J. Mao, and S.-H. Gary Chan, "A survey on deep learning-based single image crowd counting: Network design, loss function and supervisory signal," *Neurocomputing*, vol. 508, pp. 1–18, 2022, <https://doi.org/10.1016/j.neucom.2022.08.037>.
- [37] Q. Wang, Y. Ma, K. Zhao, and Y. Tian, "A comprehensive survey of loss functions in machine learning," *Annals of Data Science*, pp. 1–26, 2020, <https://doi.org/10.1007/s40745-020-00253-5>.
- [38] Y. Feng *et al.*, "A comparative study of automatic image segmentation algorithms for target tracking in MR-IGRT," *J. Appl. Clin. Med. Phys.*, vol. 17, no. 2, pp. 441–460, 2016, <https://doi.org/10.1120/jacmp.v17i2.5820>.
- [39] M. Alidoost *et al.*, "Model utility of a deep learning-based segmentation is not Dice coefficient dependent: A case study in volumetric brain blood vessel segmentation," *Intell. Med.*, vol. 7, p. 100092, 2023, <https://doi.org/10.1016/j.ibmed.2023.100092>.
- [40] D. N. Triwibowo, B. P. Dewa, B. B. Sumantri, and R. Suryani, "Identification of Breast Tumors With Image Processing Using Canny Edge Detection," *J. Adv. Heal. Informatics Res.*, vol. 1, no. 1, pp. 28–34, 2023, <https://doi.org/10.59247/jahir.v1i1.20>.
- [41] K. Y. Halim, D. T. Nugrahadi, M. R. Faisal, and R. Herteno, "Gender Classification Based on Electrocardiogram Signals Using Long Short Term Memory and Bidirectional Long Short Term

- Memory,” *J. Ilm. Tek. Elektro Komput. dan Inform.*, vol. 9, no. 3, pp. 606–618, 2023, <http://dx.doi.org/10.26555/jiteki.v9i3.26354>.
- [42] M. F. Nafiz, D. Kartini, M. R. Faisal, F. Indriani, and T. Hamonangan, “Automated Detection of COVID-19 Cough Sound using Mel- Spectrogram Images and Convolutional Neural Network,” *J. Ilm. Tek. Elektro Komput. dan Inform.*, vol. 9, no. 3, pp. 535–548, 2023, <http://dx.doi.org/10.26555/jiteki.v9i3.26374>.
- [43] F. Melky, S. Sendari, and I. A. Elbaith, “Optimization of Heavy Point Position Measurement on Vehicles Using Support Vector Machine,” *J. Ilm. Tek. Elektro Komput. dan Inform.*, vol. 9, no. 3, pp. 673–683, 2023, <http://dx.doi.org/10.26555/jiteki.v9i3.26261>.
- [44] M. Ilham, A. Prihantoro, I. K. Perdana, R. Magdalena, and S. Saidah, “Experimenting with the Hyperparameter of Six Models for Glaucoma Classification,” *J. Ilm. Tek. Elektro Komput. dan Inform.*, vol. 9, no. 3, pp. 571–584, 2023, <http://dx.doi.org/10.26555/jiteki.v9i3.26331>.
- [45] L. Marco, “Comparative Study of Optimizers in the Training of a Convolutional Neural Network in a Binary Recognition Model,” *Res. Comput. Sci.*, vol. 150, no. 4, pp. 73–82, 1870.
- [46] Z. Qu, S. Yuan, R. Chi, L. Chang, and L. Zhao, “Genetic Optimization Method of Pantograph and Catenary Comprehensive Monitor Status Prediction Model Based on Adadelta Deep Neural Network,” *IEEE Access*, vol. 7, pp. 23210–23221, 2019, <https://doi.org/10.1109/ACCESS.2019.2899074>.
- [47] J. Sharma *et al.*, “A novel long term solar photovoltaic power forecasting approach using LSTM with Nadam optimizer: A case study of India,” *Energy Sci. Eng.*, vol. 10, no. 8, pp. 2909–2929, 2022, <https://doi.org/10.1002/ese3.1178>.
- [48] D. Yi, J. Ahn, and S. Ji, “An Effective Optimization Method for Machine Learning Based on ADAM,” *Applied Sciences*, vol. 10, no. 3, 2020, <https://doi.org/10.3390/app10031073>.
- [49] E. Hassan, M. Y. Shams, N. A. Hikal, and S. Elmougy, “The effect of choosing optimizer algorithms to improve computer vision tasks: a comparative study,” *Multimed. Tools Appl.*, vol. 82, no. 11, pp. 16591–16633, 2023, <https://doi.org/10.1007/s11042-022-13820-0>.
- [50] S. A. H. Hosseini, B. Yaman, S. Moeller, M. Hong, and M. Akçakaya, “Dense Recurrent Neural Networks for Accelerated MRI: History-Cognizant Unrolling of Optimization Algorithms,” in *IEEE Journal of Selected Topics in Signal Processing*, vol. 14, no. 6, pp. 1280–1291, 2020, <https://doi.org/10.1109/JSTSP.2020.3003170>.
- [51] Y. Shen, F. Zhang, D. Liu, W. Pu, and Q. Zhang, “Manhattan-distance IOU loss for fast and accurate bounding box regression and object detection,” *Neurocomputing*, vol. 500, pp. 99–114, 2022, <https://doi.org/10.1016/j.neucom.2022.05.052>.
- [52] C. Shorten and T. M. Khoshgoftaar, “A survey on Image Data Augmentation for Deep Learning,” *J. Big Data*, vol. 6, no. 1, p. 60, 2019, <https://doi.org/10.1186/s40537-019-0197-0>.
- [53] M. Yaqub *et al.*, “State-of-the-Art CNN Optimizer for Brain Tumor Segmentation in Magnetic Resonance Images,” *Brain Sci.*, vol. 10, no. 7, 2020, <https://doi.org/10.3390/brainsci10070427>.